J. Membrane Biol. 115, 13–29 (1990)

The Journal of
Membrane Biology

Characterization of Sodium Currents in Mammalian Sensory Neurons Cultured in Serum-Free Defined Medium with and without Nerve Growth Factor

Gila Omri and Hamutal Meiri*

Department of Physiology and Biophysics, Faculty of Medicine, and The Rappaport Family Institute for Research in The Medical Sciences, Technion-Israel Institute of Technology, Haifa 31096, Israel

Summary. The influence of nerve growth factor (NGF) on Na currents of rat dorsal root ganglia (DRG) was studied in neurons obtained from newborns and cultured for 2–30 hr in *serum-free defined medium* (SFM). Cell survival for the period studied was 78–87% both with and without NGF. Na currents were detected in all cells cultured for 6–9 hr. They were also detected after 2 hr in culture in 21.5% of the cells cultured without NGF (−NGF cells), and in 91.5% of the cells cultured with NGF (+NGF cells). Current density of the −NGF cells was 2.3 and 2 pA/μm^2 after growth for 2 and 6–9 hr, respectively, compared to 3.0 and 3.9 pA/μm^2 for the +NGF cells. The+NGF cells were separated into fast (*F*), Intermediate (*I*) and slow (*S*) cells, based on the Na current they expressed, while −NGF cells were all of the *I* type. *F*, *I* and *S* currents differed in their voltage-dependent inactivation (Vh_{50} = −79, −28 and −20 mV), kinetics of inactivation (tau_h = 0.55, 1.3 and 7.75 msec), and TTX sensitivity (K_i = 60, 550 and 1100 nM). All currents were depressed by $[Ca]_o$ with a Kd_{Ca} of 22, 17 and 8 mM for *F*, *I* and *S* currents, respectively. Current density of *F* and *S* currents was 5.5 and 5 pA/μm^2 for the *I* current. The concentration-dependent curve of *I* current *vs.* TTX indicated that *I* current has two sites: one with *F*-like and another with *S*-like K_i for TTX. Hybridization of *F* and *S* currents yielded *I*-like currents. Thus, the major effect of NGF on Na currents in SFM is the accleration of Na current acquisition and diversity, reflected in an increase of either the *S* or *F* type in a cell.

Key Words nerve growth factor · dorsal root ganglia · sodium channels · patch clamp · channel development · tetrodotoxin

Introduction

The peripheral sensory neurons originate from the dorsal root ganglia (DRG), which are derived from the neural crest [35, 53]. These neurons send the nerve fibers that participate in coding sensory information into patterns of neuronal firing [12, 15, 16]. The cell bodies of myelinated fibers conducting information about touch, pressure and temperature have fast-rising, TTX-sensitive, sodium-dependent action potentials. Cell bodies of *c* fibers conducting nociceptive information tend to repetitively fire slow-rising, sodium-dependent action potentials of high threshold and low TTX-sensitivity [15, 16, 39, 40, 67]. The question is how this diverse firing pattern is developed.

Studies during the last two decades have shown developmental changes in the firing pattern and shape of the action potentials in many neurons [46, 62]. In mammalian DRG neurons, the action potentials are modified during maturation as a result of changes in their ionic currents [20, 39, 47]. One of the prominent effects is a gradual increase in the proportion of neurons with TTX-sensitive over TTX-resistant, *sodium*-dependent action potentials [20, 39]. This is consistent with the developmental changes in two types of sodium currents: a TTX-sensitive current with rapid kinetics of activation and inactivation, and a slow current with low TTX-sensitivity [31, 42]. Thus, it is important to identify the factor(s) involved in the regulation of such developmental changes.

One such potential factor is nerve growth factor (NGF). This polypeptide is one of the most fully characterized growth factors [5, 53, 58, 60], and its function is relatively well understood [5, 25, 28, 35, 36]. It is now known that in DRG neurons, like in many other cells derived from the neural crest, NGF is responsible for the selective survival of cell populations, and the subsequent maintenance of their differentiated state [35, 41, 53, 58, 60]. Interest now focuses on the molecular processes invoked by NGF, in particular its possible role in the regulation of various ion channels—mainly Ca [64] and Na [38, 48, 56]—and their development in neurons derived from the neural crest.

* *Present address:* c/o Prof. E. Landau, Department Psychiatry, Bronx VA Medical Center, 116A, 130 W. Kingsbridge Road, Bronx, New York 10468.

The present study was undertaken to examine the role of NGF in controlling the appearance of diverse sodium currents. It was conducted on DRG from newborn rats despite the fact that not all DRG cells are sensitive to NGF at this stage [35, 53]. The choice was made because newborn cells contain both fast and slow currents [31, 42] while the more NGF-sensitive embryonic cells have mostly fast Na current, at least in freshly dissociated neurons from 14–15 days embryo [68, and *manuscript in preparation*].

In the past, sodium currents were recorded in cultured DRG cells from newborn rats using intracellular perfusion [31].

The whole-cell patch-clamp technique subsequently used [14] to record Na currents from the DRG. However, patch-clamp results were given for embryonic or adult cells after growth in culture for several days, weeks and even months [40, 49], and cells were also cultured in media containing serum [31, 40, 42, 49]. The present study adapts the patch-clamp technique to freshly dissociated cells cultured for a short time in a serum-free *defined* medium (SFM) [25, 26, 41]. The properties of the Na currents of neurons cultured in SFM with and without NGF are characterized, and the role of NGF in regulating the properties and diversity of the sodium current are examined. Experimental conditions approximate physiological conditions as closely as possible, and the defined medium enables assessment of the effects of NGF.

Our major conclusions are that under the experimental conditions used here, NGF fosters earlier appearance of Na currents, larger peak current density, and the accelerated development of sodium current diversity, expressed in the early appearance of more *F* and *S* neurons than *I* neurons. Thus, NGF is demonstrated to have a role in the differentiation of the diverse pattern of currents in sensory neurons.

Materials and Methods

Cultures of Dorsal Root Ganglion (DRG) Cells

Lumbar and sacral ganglia were isolated from newborn rats (1–2 days old) and transferred into a physiological solution composed of (in mM): NaCl 136.8, KCl 2.6, Na_2HPO_4 0.28, $NaHCO_3$ 2.6, and glucose 33.3 (pH 7.3, adjusted with 1 M NaOH and osmolarity 300 mOsm). The medium was supplemented with penicillin (100 U/ml), streptomycin (0.1 mg/ml), and fungizone (0.25 μg/ml). The roots were removed and the ganglia were incubated for 30 min at 37°C with trypsin (0.05%, Difco 1:250). After extensive washing with serum-free defined medium (SFM, *see below*) to remove the enzyme, single cells were released from the ganglia by agitation with flame-polished Pasteur pipettes. Cells (10^3–10^4) were plated at homogeneous density onto 35-mm Falcon tissue culture dishes precoated with 5 μg/ml of poly-L-lysine, using 2 ml of culture medium (SFM).

The SFM consisted of Eagle's basal medium, supplemented with 2 mM glutamine (Biological Laboratories, Beit-Hamek, Israel), 0.3% glucose, 25 μg/ml insulin, 25 μg/ml transferrin [human], 100 nM cortisone, 0.07 μg/ml biotin, 1.36 μg/ml vitamin B_{12}, 30 nM 3-iodo-thrionine (T_3), 10 μM L-carnitine, 10 μM linoleic acid, and 1 μM lipoic acid (all from Sigma, St. Louis, MO). Nerve growth factor (beta-NGF, Sigma #N-0513) was added, when indicated, immediately after plating at a final concentration of 100 ng/ml. The biological activity of NGF was measured using the tissue culture bioassay of Fenton [9].

Cultures were maintained in 5% CO_2 at 37°C. After 2 hr in culture, bright neurons (10–15 μm diameter) were distinguished from the fibroblasts, Schwann cells and other cells by their round shape, bright halo and short, thin neurities.

Cell Survival

At 10 × 10 magnification of the inverted microscope, living cells were identified as those not taking trypan blue. The baseline (100% living cells) was set by measuring the percent of living cells 1 hr after culturing. To estimate this value, 100 fields of 0.5 × 0.5 mm were sampled at 2-mm distances throughout the culture dish. The sampled area was 2.6% of the entire surface area. The mean number of living cells in all 100 fields of 10–12 plates was calculated and normalized to the mean number of surviving cells measured 1 hr after culturing.

Cell Sampling for Electrophysiological Experiments

Round bright cells, 10–15 μM in diameter, were used for patch clamping. In the freshly dissociated cells (2–3 hr in culture), these neurons usually had no neurites. After 6–9 hr in culture with or without NGF these cells had neurites. Only cells with thin (below 2 μM), short (<30 μm) processes were patch clamped. After 24–30 hr in culture, sprouting of cells cultured with NGF was too vigorous to allow an appropriate space clamping. At any time of the time periods studied, the sampled cells accounted for 30–40% of the population, and all our conclusions were *limited* to this kind of cells.

When larger bright cells (25–30 μm) were occasionally patch clamped (after any culturing duration), their capacitance was too large to be appropriately space clamped with the EPC-7 amplifier used in these studies. Small dark cells (2–10 μm diameter), corresponding to *c* fibers [3], were not taken because of their fragility and difficulty in accurately defining them as neurons.

Electrophysiology

Recording Solutions

Fire-polished borosilicate electrodes (1–6 MΩ) were filled with internal solution consisting of (in mM): NaCl 10, CsCl 135, $MgCl_2$ 5, HEPES 5 and EGTA 5; Osm 290–300, pH 7.35 (adjusted with 1 M CsOH). Neurons were patch clamped in culture dishes externally perfused with EG-100 (Table 1). A perfusion system by

Table 1. Composition of external solutions

Solution	EG100$^+$	0.01 Ca	0.1 Ca	1 Ca	2 Ca	5 Ca	12 Ca
NaCl	100	80	80	80	80	80	80
KCl	5	5	5	5	5	5	5
$CaCl_2$	—	0.01	0.1	1	2	5	12
$MgCl_2$	5	5	5		5	5	5
TrisCl	—	20	20	18.5	17	5	2
TEA-Cl	40	40	40	40	40	40	40
HEPES-Na	5	5	5	5	5	5	5
Na_2HPO_4	2	2	2	2	2	2	2
Glucose	10	10	10	10	10	10	10

EG100$^+$-standard extracellular solution. All values are in mM. Osm = 290–300, pH = 7.4, adjusted with 1 N NaOH.

which the external solution could be replaced within 1 min was used for changing the composition of the external solution (Table 1) or adding TTX.

Separation of Na Current

For studying sodium currents, the K channels were blocked with tetraethylammonium ions in the external solution, and cesium in the internal solution [42]. Selective blocking of calcium channels in this preparation is not trivial. Dihydropyridins were found ineffective in blocking the various types of Ca channels in rat DRG cells [8, 30]. Cations which block Ca channels (Cd, Co) could not be used since they significantly attenuate the Na currents of this preparation [31, 42, 49]. D-600 was found to block both Ca channels and slow sodium channels [31]. Fluoride, which blocks Ca current in this preparation [30, 31], could not be used on the inside as it polarizes the recording *vs.* ground electrode [49]. Thus, the current through the calcium channels was blocked as follows: a low concentration of calcium (10 μM) was added to the external solution to block the calcium channels by calcium binding to its high affinity site within its channel [1, 8, 17, 37]. Mg^{2+}, a nonpermeable Ca competitor [17], was used on both sides of the membrane (5 mM), and EGTA was employed from inside to buffer calcium leaking from internal stores [21]. The current flowing in the calcium channels under these conditions is negligible [1, 8, 17, 37].

Current Recording

The cells were studied with a List pre-amplifier (EPC-7) with a 1 GΩ head stage set for a whole-cell clamp configuration [14]. Currents were filtered at 3–10 kHz, except for pure fast currents which were filtered at 10 kHz. Capacitative transients were minimized using the negative capacity compensation of the patch-clamp amplifier [14]. Further capacity subtraction was achieved digitally using currents elicited by depolarizing the membrane from a prepulse to −130 mV to the holding potential (−70 mV, at which all currents are inactive). This pulse was used for point-to-point subtracting of the capacitative transient after correcting for the appropriate membrane potential ($I_c = -cdV/dt$, where c is the cell capacitance and dV is the change in membrane potential at any given time, dt).

The series resistance, R_s, mainly due to the microelectrode resistance, was uncompensated to avoid oscillations of the amplifier which damage the cells [49]. Because of this, the error in the voltage applied to the membrane was estimated by attenuating sodium current with TTX. The attenuated sodium current was not shifted along the voltage axis, indicating that the series resistance error was negligible [51, 63]. The holding potential (V_H) was −70 mV. A Data General "Desk top-30" computer with analog-to-digital and digital-to-analog converters was used to generate command voltages, and to digitize the currents at sampling rates of 2–24 kHz at 10-bit resolution.

Leakage Subtraction

In the absence of K and Ca currents, leakage current was considered to be the steady-state current remaining after suppression of the TTX-sensitive fast sodium channel with 300 nM TTX, or of the less sensitive slow sodium channel by 30 μM TTX. Alternatively, the leakage current (I_L) was measured during a 40-mV hyperpolarizing pulse, and the leakage conductance (G_L) was calculated. Leakage current at any V_m was calculated assuming a linear leakage I/V relationship and that $E_L = -70$ mV. In most experiments the leakage current was calculated according to the latter method. Experiments in which leakage conductance exceeded 5% of peak sodium conductance were rejected.

I/V Curves

Membrane potential (V_m) was stepped by a 40-msec prepulse to −110 mV followed by 40-msec command pulses to V_m values between −60 and +90 mV in 5–10 mV increments. Pulses were applied at intervals of 4 sec. The peak sodium current (peak I_{Na}) was measured at various V_m's. The current reversal potential (E_r) was determined from the I/V curve. The current density was computed by dividing the measured peak I_{Na} by the cell surface area. The latter was estimated from measurements of cell capacitance (*see below*).

Relative Conductance

Peak sodium conductance $\{g_{Na}(\max)\}$ at every V_m was calculated from $g_{Na}(\max) = I_{peak}/(V_m - E_r)$. The $g_{Na}\max$ values obtained at each V_m were then normalized to the largest $g_{Na}\max\{g_{Na}(\text{bar})\}$ to obtain the relative conductances which were then plotted as a function of V_m.

Table 2. Electrophysiological parameters of sodium currents in neurons grown with and without NGF

	Without NGF (n = 13)	With NGF		
		Intermediate (n = 13)	Slow (n = 6)	Fast (n = 6)
V_m (mV) at I_{Na} peak	−11.6 ± 7.4	−10.5 ± 7.2	−10.0 ± 1.0	−26.6 ± 2.0**
Peak current density (pA/μm^2) (n = 5)	2.5 ± 1.3	2.0 ± 0.3	5.0 ± 1.3**	5.5 ± 1.8**
E_r (mV)	57.9 ± 5.4	57.5 ± 3.2	61.0 ± 3.0	66.0 ± 7.4
Vh_{50} (mV)	−32.0 ± 8.0	−28.7 ± 5.1	−20.5 ± 3.0	−70.2 ± 8.6**
Vg_{50} (mV)	−27.0 ± 11.0	−28.7 ± 3.0	−23.7 ± 1.1	−43.0 ± 4.2**
Slowest tau$_h$ (msec)	1.5 ± 0.6 (V_m = −25 mV)	1.3 ± 0.4 (V_m = −25 mV)	7.75 ± 1.7** (V_m = −25 mV)	0.55 ± 0.3* (V_m = −35 mV)
Slowest tau$_m$ (msec)	—	—	0.7 ± 0.2 (V_m = −20 mV)	—
Living cells (%) (at 24 hr)	78 ± 7	87 ± 8 (for all +NGF cells)		

Measurements were taken at 6–9 hr after culturing. Values are means ± SD. All values of the intermediate current of the +NGF cells were indistinguishable from the current of −NGF cells. The fast and slow current have parameters, which (when indicated) are significantly different from either the intermediate current of +NGF cells or the current of the −NGF cells.
* $P < 0.05$.
** $P < 0.01$ for two-tailed t test.

Current Inactivation

The sodium current inactivation was determined as a function of V_m by pairs of pulses, each composed of a 40-msec conditioning prepulse to various potentials (V_{pp}), followed by a 40-msec test pulse to V_m = +10 mV. The ratio between I_{peak} obtained following any prepulse potential, and the maximal I_{peak} (h_{inf}), was plotted against V_{pp}.

Kinetics of Activation

The time constant of activation (tau$_m$) was computed from the slope of $\log(I_{inf} - I_t)$ *versus* t (where I_{inf} is the current at the peak and I_t is the current at any time before the peak). The slope (1/tau$_m$) was linear, indicating a single exponential function of time. The tau$_m$'s obtained for various depolarization pulses were then plotted against V_m to obtain the typical bell-shaped curve. The slowest tau$_m$ was obtained from the peak of the bell curve.

Kinetics of Inactivation

The time constant of inactivation (tau$_h$) was computed from the $\log(I_{inf} - I_t)$ versus t (where I_{inf} = the current at t − > inf and I_t = the current at any t from the peak). The slope (1/tau $_h$) was linear, indicating a single exponential function of time. The tau$_h$ were then plotted against V_m to obtain the bell curve, from which the slowest time constant of inactivation was obtained.

Measurements of Cell Capacitance

The cell membrane capacitance (C_m) was measured by means of the triangular waveform method [50] adapted to patch clamp. The membrane potential was centered at the holding potential (−70 mV), and triangular 230 Hz waveform was given. Since size of the waveform (peak-to-peak amplitude $-V_0$) was 25 mV (i.e., 12.5 above and below the holding potential), the triangular pulse did not initiate Na currents. Note that Ca and K channels were already blocked at the external and internal solutions used here. The cell capacity was computed from $c_m = I_0 w/4V_0$, where I_0 is the peak-to-peak current, and w is the wavelength of the triangular wave. The cell surface area could be calculated as the ratio between cell capacitance, c_m, divided by the specific capacitance of 1 cm^2 of a cell membrane (C_m). The latter was taken as 1 μF/cm^2, a typical value for biological membranes. This value is known to be similar in numerous types of cells from a variety of tissues and species, regardless of their phospholipid composition [21, 51]. Thus, it was assumed that the specific membrane capacitance C_m would be the same at various growth conditions and that all changes in the whole-cell membrane capacitance (c_m) are due to changes of the cell surface area.

Results

DRG neurons were found to survive and grow neurites in serum-free medium (SFM) with and without NGF [38]. Under both conditions, most neurons (78–87%) survived the first 24–30 hr in culture (Table 2). Patch clamping was feasible beginning 2 hr after culturing. Measurements were taken at 2, 6–9 and 24–30 hr. The outgrowth of cells cultured with NGF at 24–30 hr was too vigorous to allow adequate space clamping (*see* Table 4).

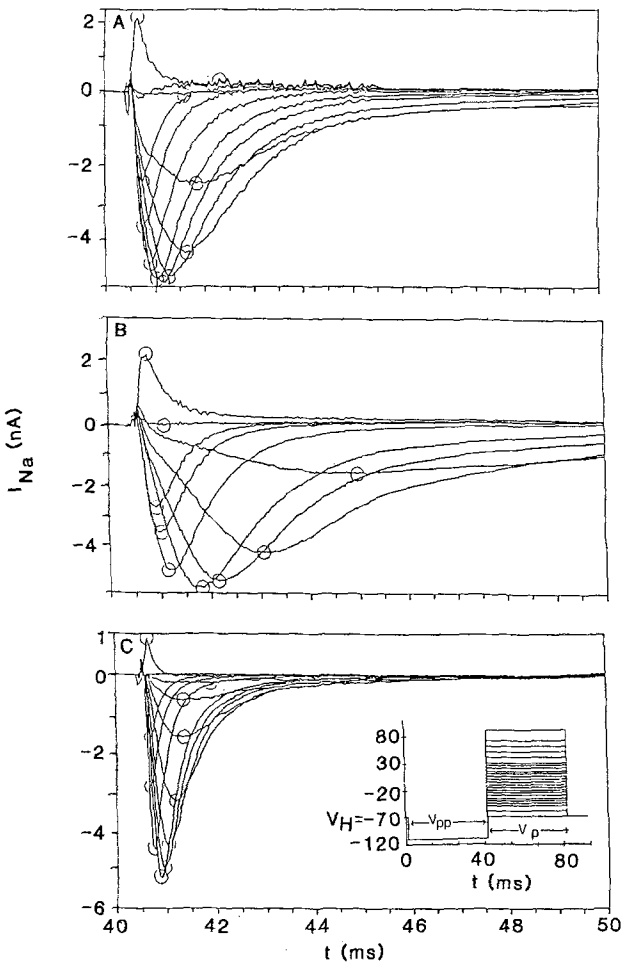

Fig. 1. Three types of Na current in DRG neurons grown in SFM with NGF. Representative current traces at various membrane depolarizations generated in (*A*) intermediate cell, (*B*) slow cell and (*C*) fast cell. Inset: stimulation protocol. V_H—holding potential, V_{pp}—pre-pulse potential and V_p—test pulse potential. All membrane potentials are given in relation to V_{out} = 0. Traces were filtered at 3 kHz in *A* and *B*, and at 10 kHz in *C*. Cells were cultured for 6–9 hr with NGF

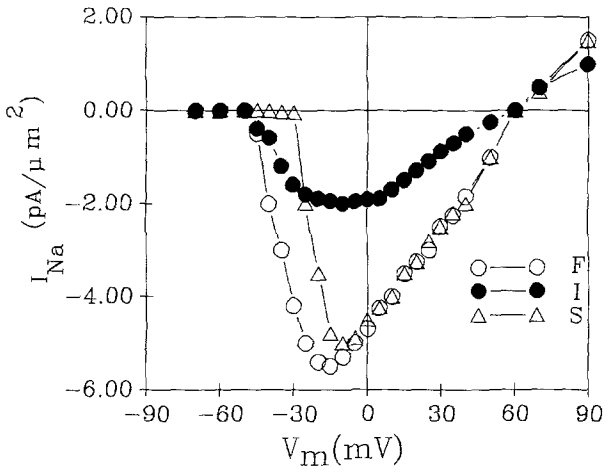

Fig. 2. Current-voltage relationship. Peak sodium current density at different V_m's as plotted against V_m for *F* (open circles), *I* (filled circles) and *S* (open triangles) currents is shown for the traces of the cells described in Fig. 1

Characterization of the Voltage Dependency and Kinetics of Sodium Currents in DRG Cells Grown in SFM with or without NGF

NGF-Treated Cells

Three types of Na currents were identified in freshly dissociated DRG neurons cultured in the presence of NGF: *F* (fast), *I* (intermediate) and *S* (slow). Each type is found alone in single cells, named accordingly, and each type has different voltage dependency and gating kinetics (Fig. 1*A–C*). The *F*, *I*, and *S* cells, however, were morphologically indistinguishable. While *F* and *S* currents were previously reported for DRG cells cultured in the presence of serum [31, 40, 42, 49], cells with "pure" *F* or "pure" *S* currents were minor in the population, and most cells had a mixture of *F* and *S* currents within a single neuron. Growth in SFM with NGF yielded a large number of cells, each with a single current type, facilitating the characterization of these currents, as follows:

Fast Current. This extremely rapid current was activated at V_m above −45 mV, and reversed at V_m = 66 ± 7.4 mV (Fig. 2 and Table 2), approximating the Nernst equilibrium potential for sodium (E_{Na} = +60 mV). Peak current density (5.5 ± 1.8 pA/μm^2) was reached at −26.6 ± 2 mV (Fig. 2 and Table 2).

The slope of *F* current inactivation was gradual. It approached saturation at V_{pp} = −130 mV; the approximate 50% inactivation (Vh_{50}), calculated by normalizing all currents to the current obtained at V_{pp} = −130 mV, was reached at −70.2 ± 8.6 mV (Fig. 3*B* and Table 2), and the current was completely inactivated at −(24 ± 7) mV. A single time constant of inactivation (tau_h) was measured at each membrane potential. This time constant was voltage dependent with a typical bell shape of tah_h *versus* V_m [24]. The membrane potential with the slowest inactivation kinetics was found to be −35 mV (tau_h = 0.5 ± 0.3 msec) (Fig. 4*B*). Faster tau_h's were measured at larger and smaller depolarizations. Limited by the frequency response of the EPC-7, the most rapid tau_h (achieved at V_m > 50 mV) that could still be measured accurately was 0.2 msec.

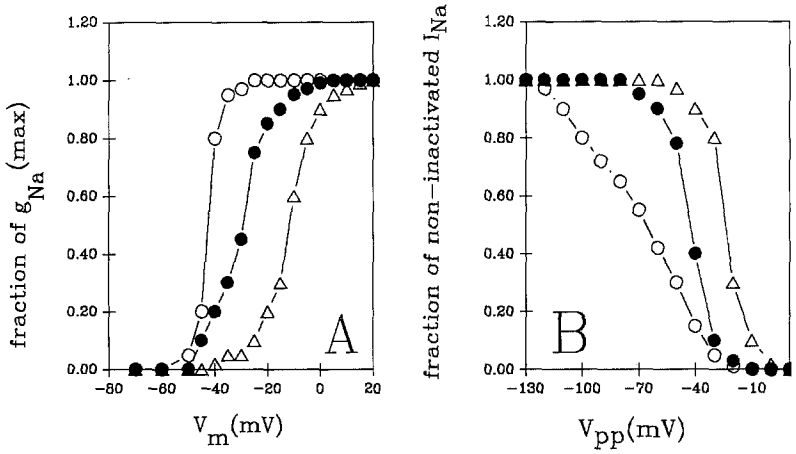

Fig. 3. Voltage dependency of activation and inactivation. (*A*) The steady-state curves of relative sodium conductance $\{g_{Na}/g_{Na}(max)\}$ for *F* (open circles), *I* (filled circles), and *S* (open triangles) currents were plotted against V_m. (*B*) The steady-state curves of sodium current inactivation $\{I_{Na}/I_{Na}(max)\}$ of *F*, *I* and *S* currents (symbols as above) plotted against V_{pp}

The relative conductance steeply increased with membrane depolarization, and reached half maximum (Vg_{50}) at $V_m = -43 \pm 4.2$ mV (Fig. 3*A* and Table 2). The kinetics of current activation were extremely rapid, and could not be measured accurately with the EPC-7.

Slow Current. The *S* current was activated at V_m above −30 mV, and reversed at $V_m = +61 \pm 3$ mV (at around E_{Na}, Fig. 2). The average peak current density, which was achieved at -10 ± 1 mV, was 5 ± 1.3 pA/μm^2 (similar to that measured for the fast current) (Fig. 2 and Table 2).

The inactivation curve steeply decreased with depolarization, and the Vh_{50} was more positive (-20 ± 3 mV) compared to the *F* currents (Fig. 3*B*). A single time constant of inactivation was measured at each membrane potential. The slowest tau_h, measured at $V_m = -25$ mV (Fig. 4*B*) was 7.75 ± 1.7 msec (over 10 times slower than the slowest tau_h of fast current). The relative conductance began to increase at V_m above −25 mV (30 mV more depolarized compared to the activation of the fast current), and reached 50% of its maximum at $V_m = -23.7 \pm 1.1$ mV (Fig. 3*A* and Table 2). The kinetics of activation was slow enough to be measured. A single time constant was obtained at each V_m. The slowest time constant of activation ($tau_m = 0.7 \pm 0.2$ msec) was reached at $V_m = -20$ mV (Fig. 4*D*).

Intermediate Current. The *I* sodium current was activated at depolarizations above −40 mV, and reversed at $V_m = 57 \pm 3.2$ (i.e., at E_{Na}, Fig. 2 and Table 2). The current density was significantly smaller compared to fast and slow currents, with the averaged peak current density (which was achieved at $V_m = -10.5 \pm 7.2$) only 2 ± 0.3 pA/μm^2 (Fig. 3 and Table 2).

The voltage dependency of sodium current inactivation and activation was steep, and the s-shaped curves reached half-maximum at membrane potentials of -28.1 ± 5.1 mV (Vh_{50}) and -28.7 ± 3 mV (Vg_{50}) (Fig. 3*A* and *B*). The kinetics of *I* current activation were too rapid to be measured accurately. The slowest tau_h (1.3 ± 0.4 msec) was measured at $V_m = -20$ mV (Fig. 5*A*); it was five times faster than the slowest tau_h of the slow current (although being measured at the same V_m), and more than two times faster than the slowest time constant of the fast current (Table 2).

NGF-Free Cells

The sodium current recorded in all cells examined after 6–9 hr of growth without NGF were of the *I* type. The voltage dependency and kinetics of the current in the −NGF cells (Fig. 5*A–C*) were indistinguishable from the intermediate current of +NGF cells (Fig. 1*A*, Fig. 2 and Fig. 3 *A* and *B*, filled circles, and pooled values in Table 2). Note, however, that the mean parameters of the *F* and *S* currents of the +NGF cells were significantly different from the current of −NGF cells (Table 2).

Current densities of the −NGF cells were similar to those of the *I* cells from the +NGF group. As described in the Materials and Methods section, current density was estimated by the measured whole-cell capacitance (c_m) divided by the specific value of the membrane capacitance (C_m). Since C_m was found constant and indifferent to growth conditions, cell age, species and tissue [21, 50], it is expected that this value would not be altered by the minor modification in cell membrane composition induced by NGF [52, 60]. Thus, the similar densities recorded for the *I* current of +NGF and −NGF cells seem to be a true reflection of the current densities, and cannot be attributed to inappropriate estimation of the cell surface area.

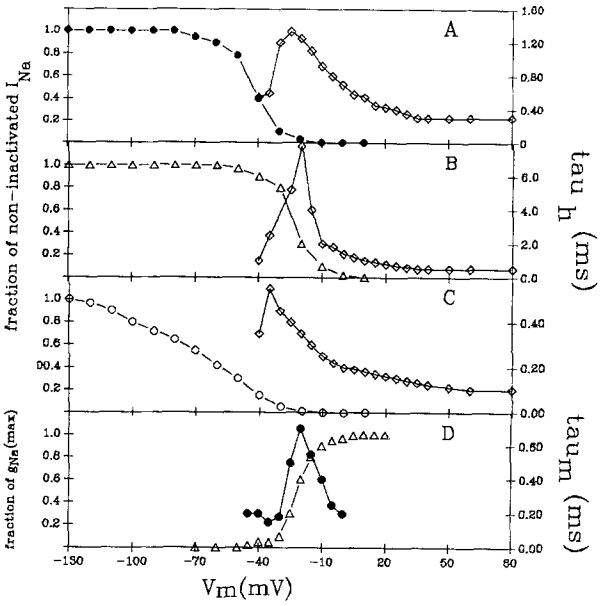

Fig. 4. Kinetics of activation and inactivation. (*A–C*) Time constants of inactivation (tau_h, open diamond symbols) of *I* (*A*), *S* (*B*) and *F* (*C*) currents are shown in relation to steady-state inactivation (symbols as in Figs. 2 and 3). Results in *A* and *B* were obtained after filtration at 3 kHz, and in *C* after filtration at 10 kHz. (*D*) Time constant of activation (tau_m, filled circles) and the relative conductance (g_{Na}/g_{Na}(max), open triangles) of *S* currents plotted against membrane potentials (V_m). The values for *F* and *I* currents were too rapid for the EPC-7. All cells examined were taken after 9 hr in culture

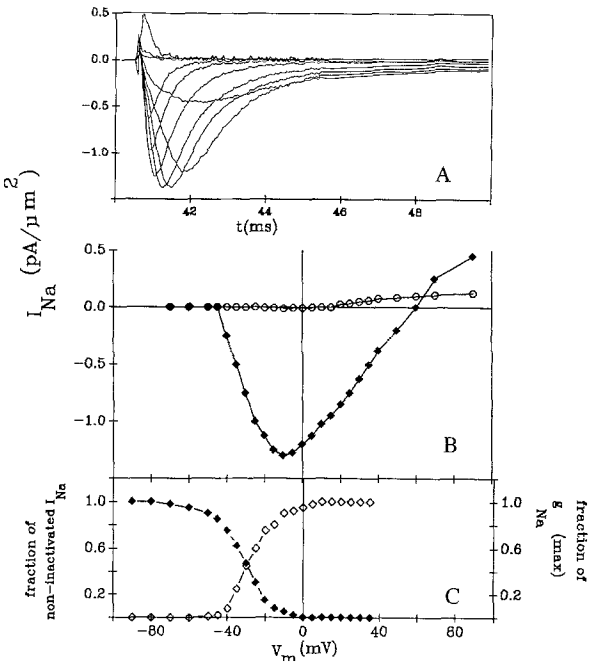

Fig. 5. Sodium current of DRG cells grown in SFM without NGF. (*A*) Current traces *vs.* time at various membrane potentials. (*B*) *I–V* curve of peak (filled diamonds) and steady-state (open triangles) currents prepared from the traces shown in *A*. (*C*) The steady-state curves of relative conductance (open diamonds) and inactivation (filled diamonds) plotted against membrane potentials. The cell was taken after 9 hr in culture

Pharmacological Characterization: Sensitivity to TTX and External Ca

The pharmacological characterization of the sodium currents was examined in neurons cultured for 6–9 hr with and without NGF.

The reversal potential (Table 2) measured for each type of current described in this study (*S*, *F* and *I*) was close to the calculated Nernst equilibrium potential (−60 mV). Furthermore, *F*, *I* and *S* currents disappeared after substitution of sodium in the external solution with the nonpermeable cation choline or Tris (*not shown*), indicating that these three currents are carried by sodium ions. In order to prove that these currents are passing through a sodium and not a calcium channel, the effects of TTX and calcium were studied.

TTX Sensitivity

+NGF Cells. It was previously found [31], and confirmed here, that the *F* current could be blocked by 0.1–0.3 μM TTX (*see* Fig. 6*A* and *D*). The concentration required to block this current by 50% (K_i) was 60 nM (Table 3). This high TTX sensitivity, together with current reversal-potential dependence on $[Na^+]_{out}$, and the dependence of peak I_{Na} on $[Na^+]_{out}$, were all taken as strong indications that the *F* currents flow through sodium channels.

The *S* current was relatively resistant to TTX, as already described by Kostyuk et al. [31], and the K_i was found to be 1.2 μM (Table 3).

The *I* current has an intermediate sensitivity to TTX, and the K_i was 550 nM. However, the concentration-dependent curve of current decrease *vs.* TTX concentration indicated the presence of two sites—one at the range of *F* current and another at the range of *S* current (Fig. 6*D*). This implies that the *I* current can be a composite of *S* and *F* currents (*see* later Fig. 7).

−NGF Cells. TTX sensitivity of the *I* current (the one available after 6–9 hr growth in −NGF cells) was virtually no different than the TTX sensitivity of the *I* current in the +NGF cells (Table 3), suggesting that TTX sensitivity does not depend on NGF.

Table 3. The effects of external calcium and TTX on the three types of Na currents

	Cells			
	Without NGF	With NGF		
	Intermediate current (n = 4)	Intermediate current (n = 5)	Fast current (n = 5)	Slow current (n = 7)
K_i TTX [μM]	0.62 ± 0.42	0.55 ± 0.34	0.06 ± 0.02**	1.10 ± 0.35*
Kd_{Ca} [mM]	15 ± 9	17 ± 6	22 ± 7	8 ± 4**
K_i TTX + 2 mM Ca	not measured	0.40 ± 0.20	0.10 ± 0.03**	0.77 ± 0.2**

K_i and Kd_{Ca} were the concentrations required to attenuate the peak of the inward current by 50%. For fast and intermediate currents K_i's were measured from the complete dose-response curves. The K_i for the slow current and all Kd_{Ca} were approximated by extrapolation of the linear curve of the current *vs.* concentration to zero. Values are means ± SD. Statistical differences were compared to intermediate current without NGF.

*$P < 0.01$.

**$P < 0.002$, for two-tailed t test.

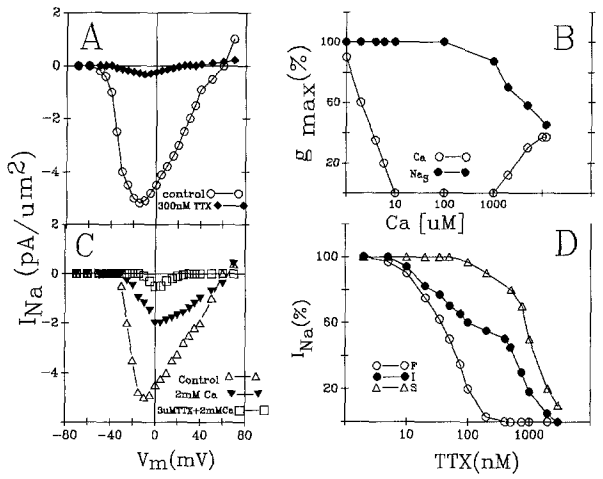

Fig. 6. The effect of TTX and $[Ca]_{out}$ on sodium currents. (*A*) *I–V* curves of *F* sodium current before (open circles) and after (filled diamonds) the addition of 300 nM TTX. (*B*) Maximal conductance of the *S* current *vs.* $[Ca]_{out}$. Filled circles—experimental g_{bar}'s measured from seven cells with *S* currents at various $[Ca]_{out}$. Open circles—values derived from references 8, 17, 31 for the behavior of the high threshold Ca channels *vs.* $[Ca]_{out}$. (*C*) *I–V* curve of *S* sodium current in normal solution (open triangles), after elevating $[Ca]_{out}$ to 2 mM (filled triangles), and at combination of 3 μM TTX with 2 mM $[Ca]_{out}$ (squares). The attenuated current obtained with 2 mM $[Ca]_{out}$ is shifted to the right, indicating that the effect cannot be a result of series resistance error. The E_{Na} of the attenuated current is not affected. Note the complete blockade of the *S* current with TTX when given in the presence of 2 mM $[Ca]_{out}$. (*D*) Concentration-dependent block of peak I_{Na} by TTX. Open circles—fast current, filled circles—intermediate current and triangles—slow current. Each curve was measured in a single cell. Note the appearance of two slopes in the *I* current. All cells examined were cultured for 6–9 hr

Calcium

It has been shown that the *S* sodium current can be blocked by D-600, cobalt and cadmium [31, 49]. This unusual pharmacology together with the low TTX sensitivity led us to check whether the *S* current flows through Ca or Na channels. We measured the effect of extracellular concentration of calcium on the *S* current.

The logic of these experiments is based on the dual effect calcium has on the calcium channel. In the absence of calcium, the calcium channel transports sodium ions. This Na transport can be blocked by micromoles of $[Ca]_{out}$ [1, 8, 30]. On the other hand, with millimoles of $[Ca]_{out}$, the block is removed and Ca ions flow through the Ca channel in a concentration-dependent manner (as illustrated in Fig. 6*B*, open circles). The decrease in calcium channel conductance to sodium by micromoles of calcium has been attributed by Hess et al. [17] to the high affinity binding of the calcium ions to a site within its channel; at millimoles of $[Ca]_{out}$, the block is removed, and the Ca ions flow through their channel as determined by a second, low affinity site in the channel [17]. Similar behavior was found by Almers and McCleskey [1], who proposed that calcium binding to a high affinity site within the calcium channel increases the energy barrier for cations fluxing through the calcium channel, which is removed at large calcium concentration [1].

Based on these characteristics of the Ca channel, three sets of experiments were designed to eliminate the possibility that the *S* current described

in this study is passing through one of the Ca channels.

+NGF Cells. In the first series of experiments, calcium was added to the extracellular solution at micromolar concentrations (1, 10 and 100 μM, Table 1). Na currents through calcium channels [8], or through the "nonselective" channel [1], were expected to be blocked in these conditions. But, the experimental results (Table 3) showed that the peak of maximal conductance of the *S* current (Fig. 6*B*) was not affected by micromoles of $[Ca]_{out}$, indicating that *S* current is not flowing through a calcium channel. The TTX-sensitive *F* and *I* currents were also not affected by micromoles of external calcium (Table 3).

In a second series of experiments, the inward current was measured before and after elevating $[Ca]_{out}$ to 1–12 mM at a constant concentration of extracellular sodium ions. Figure 6*C* summarizes such an experiment for the *S* current, showing that the peak of the *S* current (and in fact, the peak of *F* and *I* currents as well, Table 3) was depressed when $[Ca]_{out}$ was elevated from 1 to 12 mM (Fig. 6*C* and Table 3). Kd_{Ca} was the concentration required to attenuate the inward current by 50%. The Kd_{Ca} was 8 mM for *S* current, 17 mM for *I* current, and 22 mM for *F* current (Table 3). These are the results expected from a sodium channel modified by calcium [23].

Very different behavior was seen when the effect of $[Ca]_{out}$ on DRG Ca currents was examined [8, 30, 31]. The $[Ca]_{out}$ effect on our slow current was also different from the effect of $[Ca]_{out}$ on the muscle "nonspecific" channel [1].

The peak current was shifted towards depolarizations (Fig. 6*C*) in accordance with the classical effect of $[Ca]_{out}$ on peak sodium current via the surface charge [23]. A calcium effect on Na channel gating can also account for some of these effects [49]. The shift of the *I–V* curve towards depolarization occurred only with Ca, and not with TTX, although both attenuated the current, precluding a series resistance error as a possible explanation of the shift of the *I–V* curve by calcium [51, 63].

In the third set of experiments, TTX was added after attenuating Na current with millimoles of $[Ca]_{out}$. In the case of the *S* current, combining 2 mM calcium with 3 μM TTX was followed by a complete block of the *S* current (Fig. 6*C*), suggesting that external calcium elevates the affinity of *S* channel to TTX (Table 3). This is surprising considering the ability of external calcium to compete with TTX on the binding to the classical Na channel [18, 22]. In any event, the larger blocks of *S* current by TTX in the presence of millimoles of calcium serves here as another indication that *S* current is not flowing through a calcium channel.

The effect of external calcium on TTX sensitivity of the *F* current was opposite of the effect found for the *S* current. The *F* current K_i for TTX is increased from 60 to 100 nM when TTX is given with 2 mM $[Ca]_{out}$, as was previously described for other TTX-sensitive Na currents [18, 22].

These three sets of experiments strongly indicated that the *S* current is flowing through sodium channels (of low TTX sensitivity), and not through calcium channels.

−NGF Cells. The results presented in Table 3 and Fig. 6 were measured in neurons cultured for 6–9 hr. At this time, the only current available for measurements in the −NGF group was the *I* current. The effect of extracellular calcium on the *I* current of −NGF cells (Table 3) was identical to the effect of $[Ca]_{out}$ on the +NGF *I* current (Table 3), providing further evidence that once the properties of a current are established, they are not affected by NGF.

Distribution of Current Type in Cells

+NGF Cells

Table 4 summarizes the type of current in 59 +NGF cells tested at various time intervals. With the exception of two cells cultured for 2 hr, all cells cultured with NGF had Na currents. The proportion of *F* and *S* cells is increased from 2 to 6–9 hr. At 24–30 hr of culturing, currents were initiated in all examined cells, but their actual characterization was based on TTX sensitivity and not on current characterization, which was impossible to achieve due to inadequate space clamping (Table 4). At any given time, one could never tell from the morphological appearance of a cell whether it was *F*, *S* or *I* type.

−NGF Cells

A total of 47 cells were examined. Unlike cells cultured with NGF, most freshly dissociated cells cultured without NGF for 2 hr had no sodium currents at all (Table 4). After 6–9 hr of growth without NGF, all cells expressed Na current of the *I* type. After 24–30 hr in culture the *S* and *F* cell types were found among the −NGF cells (Table 4). Thus, the rate of appearance of each type of Na current, and the rate of development of current diversity, are accelerated by NGF, but NGF is not essential for *S* and *F* current appearance.

Table 4. Frequency distribution of fast, slow and intermediate cells as a function of culturing duration with and without NGF

Current type		hr in culture 2 hr		6–9 hr		24–30 hr	
		+NGF	−NGF	+NGF	−NGF	+NGF[a]	−NGF
With trypsin	*F*	2 (9.5%)	—	6 (21.4%)	—	4 (40%)	1 (6.25%)
	I	14 (66.7%)	4 (21.5%)	16 (57.1%)	13 (100%)	1 (10%)	13 (81.25%)
	S	3 (14.3%)	—	6 (21.4%)	—	5 (50%)	2 (12.5%)
	NC	2 (9.5)	14 (79.5)	—	—	—	—
Cell total no.		21	18	28	13	10	16
Without trypsin	*F*			4 (19%)	—		
	I			13 (62%)	6 (100%)		
	S			4 (19)	—		
Cell total no.				21	6		

Cultures were prepared with and without prior exposure of the ganglia to trypsin. NC = no current.
[a] Identification of the current was made on the basis of TTX sensitivity, since vigorous sprouting precluded space clamping.
The differences in the frequencies of the current types (*F*, *I*, *S* or NC) between each NGF group and its matched −NGF group were all significant ($P < 0.001$) as determined by the chi-square test. The frequency differences between the three +NGF groups cultured for different durations were significant ($P < 0.02$). The three −NGF groups were also significantly different in current type distribution ($P < 0.001$). There were no significant differences between the cells prepared with and without trypsin after 6–9 hr in culture with or without NGF.

Time-Dependent Changes in the Properties of the Currents

The properties of the *I* current were virtually identical in all −NGF and +NGF cells, regardless of culturing duration (*not shown*). Characteristics of *S* and *F* currents identified in the +NGF cells were similar at 2 and 6–9 hr (*not shown*). The properties of *S* and *F* currents of the +NGF and −NGF cells were also the same (*not shown*). Note, that cell survival for the first 24 hr in culture with and without NGF was similar (Table 2). This is consistent with the conclusion that the properties of a particular current once established are not NGF dependent. Properties and densities of *S* and *F* currents in the +NGF cells at 30 hr were not determined because of difficulties in space clamping (*see* Materials and Methods).

Current Density

The mean Na current density of all cells with Na current (regardless of type) was larger in the +NGF group than in the −NGF group. This was true at both 2 and 6–9 hr (Table 5). This difference is due mainly to the increased frequency of cells with *S* and *F* currents (Table 4), since the latter have twice the current density of cells with *I* current (Table 5). Thus, the NGF-accelerated appearance of cells with either *F* or *S* sodium currents is partly related to evoking the appearance of cells with a larger sodium current density.

Current density of *S* and *F* cells in the +NGF cells were not altered between 2 and 6–9 hr (Table 5), indicating that the density of these currents once established in a cell are not dependent on the duration of the exposure to NGF.

The density of the *I* current in the +NGF and −NGF groups 6–9 hr after culturing were identical, but *I* current was significantly larger for cells cultured without NGF for 30 hr than for 9 hr (Table 5). This may indicate that if *I* current remains in cells for long enough—its current density is eventually increased. Unfortunately, it was impossible to obtain the comparable value for the +NGF group, due to poor space clamping.

Acute Effect of NGF

Cell survival in the +NGF and −NGF groups was similar. Since cell division in both groups is limited, the increased frequency of *F* and *S* cells, and the decreased frequency of *I* cells, might indicate that the *I* cells are turned *S* or *F*. We tried following such an event in a single cell.

Freshly dissociated neurons cultured in SFM

Table 5. Peak current density (pA/μm^2) of neurons cultured with and without NGF

hr in culture	−NGF (*I* only)	+NGF (all cells)	*F*	*S*	*I*
2	2.3 ± 0.8 ($n = 4$)	3.3 ± 0.7[a] ($n = 19$)	5.1, 4.7 ($n = 2$)	5.0 ± 0.8 ($n = 3$)	1.8 ± 0.7 ($n = 14$)
6–9	2.0 ± 1.1 ($n = 10$)	3.9 ± 0.7[b] ($n = 28$)	5.5 ± 1.8 ($n = 6$)	5.0 ± 1.3 ($n = 6$)	2.0 ± 0.3 ($n = 16$)
30	3.3 ± 0.6[a] ($n = 5$)	—			

Values are means ± SD. In the −NGF group all cells examined were of the intermediate (*I*) type. The +NGF cells are presented first as the pooled mean value (under column all cells), and than subdivided into the fast (*F*), slow (*S*) and *I* groups. For statistical significance, values of all cells in the +NGF group were compared to the −NGF cells using two-tailed *t* test.
[a] $P < 0.05$.
[b] $P < 0.01$.

for 2 or 6–9 hr without NGF were patch clamped, identified usually as *I* cells but occasionally as *S* or *F* cells and then perfused with 100 ng NGF/ml external solution. NGF had no effect on either *F*, *S* or *I* currents. Conclusions are limited, however, by the experimental conditions: the cells could be held for only 45 min—perhaps, too short a time to allow NGF to transfer one current type into another; the experimental temperature was 20 not 37°C, which might have delayed the development of an NGF effect; and only 28 cells were examined, all of which could conceivably (although not very likely) have been NGF insensitive. Moreover, essential cellular components might have been lost during cytoplasm perfusion with the patch electrode.

What Are *I* Currents?

Further characterization of *I* current focused on testing three hypotheses: (*i*) that *I* current is an immature form of Na current, which is later replaced by *F* and *S* currents; (*ii*) that *I* current is the current developed in NGF-insensitive cells [19]; and (*iii*) that *I* current is a "modified" current, an artifact of the exposure of the ganglia to trypsin [34].

The last option was studied first. Ganglia were isolated as described earlier, but instead of exposing them to trypsin, each ganglion was dissected into four pieces and the cells were released mechanically by agitation with a flame-polished Pasteur pipette. The yield was smaller, but in cells cultured for 6–9 hr, the frequency of each current type in the +trypsin and −trypsin cultures was practically identical in the +NGF and −NGF groups (Table 4). These results proved that the *I* current is not generated by trypsin-digesting parts of the Na channel [34], and that the distribution of current types among the DRG cells could not be attributed to trypsin modifying the responsiveness of DRG cells to NGF (that is, the *I* cells are not those that lost their NGF receptors as a result of trypsin digestion).

Cells were then treated in SFM+NGF for 9 hr, followed by 9 hr of SFM−NGF. Comparison of the frequency of cell type obtained under these conditions (Table 6) to that obtained in cultures grown for 18 hr with or without NGF, showed that the fraction of *F* and *S* cells was directly proportional to the duration of growth with NGF (Table 6). Thus, although we were unable to turn *I* cells into *F* or *S* cells (and vice versa), such a turning is most likely happening. The *I* current found in cells after 18 hr in culture is therefore the current of cells which are late to respond to NGF or those which never turn *F* or *S*. The latter possibility is supported by the finding that *I* current density in −NGF cells is larger at 30 hr than at 6–9 hr (Table 5).

A final experiment examined the possibility that in view of the sensitivity of the *I* current to TTX (Fig. 6*D*), this current is actually a mixture of *F* and *S* currents. Current traces of *F* cell (Fig. 7*A*, smooth line) and of *S* cell (Fig. 7*A*, dashed-dotted line) were mixed at 1 : 1 ratio (dotted line, Fig. 7*A*). The resultant "hybrid" traces obtained at each membrane depolarization (Fig. 7*A* and *B*) were similar to the *I* current traces recorded experimentally in *I* cells of the −NGF (Fig. 7*C*) and +NGF (Fig. 7*D*) cells. The differences can be attributed to the ratio of the mixture, which in nature can be other than 1 : 1 (inset of Fig. 7). This analysis does not prove that the *I* current is not a separate current entity, but taken together with the finding that TTX sensitivity of *I* current can be mediated by two sites corresponding to *F* and *S* channels, speaks strongly against the separate entity of *I* current. Single-channel analysis is

Table 6. The effect of culturing duration with NGF on the frequency of fast, intermediate and slow cells

Current type	DRG cells		
	18 hr −NGF	9 hr +NGF → 9hr −NGF	18 hr +NGF
Fast	4	6	8
Intermediate	14	9	6
Slow	2	5	6

Cultures were grown for either 18 hr without NGF, 9 hr with NGF followed by 9 hr without NGF, or 18 hr with NGF. Five dishes were prepared in each group, and four cells (10–15 μm in diameter) were arbitrarily selected at the center of each dish. The frequency of the current types (fast, intermediate or slow) differed significantly between the three experimental groups ($P < 0.01$) as determined by the chi-square test for three samples of 20 cells each.

required to identify the final number of channel types in these cells.

Further analyses have shown that at an $F:S$ ratio of 8 : 1, the current is practically a pure F current; and at an $F:S$ ratio of 1 : 5, the cell is practically a pure S cell.

Discussion

Current Characterization and Its Relevance to Firing Diversity

The diversity of sodium currents in rat DRG cells, and the presence of fast (F) and slow (S) currents, have been described [3, 30, 31, 40, 42, 49]. A complete current characterization was usually difficult to obtain, since most newborn and adult neurons contain a mixture of F and S currents within a single cell [31, 40], requiring separation by pharmacological and electrophysiological procedures. Our approach of growing DRG cells in serum-free defined medium in the presence of NGF yielded a large proportion of cells with either F or S currents, thereby simplifying the characterization of each current.

Our findings differed from those of Orozco et al. [49], who cultured embryonic cells for 2–3 weeks. Their activation and inactivation curves were shifted to more depolarized values, and their slopes of the activation and inactivation curves were steeper, due in part to their use of cobalt and cadmium to block the S current and characterize the F currents in mixed cells. Our results also differ from those of Kostyuk et al. [31], whose kinetics of current inactivation were 10 times slower for the F current and two times slower for the S current than ours. In addition, our inactivation curves were 10 and 30 mV more depolarized than theirs for the F and S currents, respectively. These differences can be attributed to different techniques, and their use of Tris *versus* our use of cesium as the major cation in the internal solution [31]. These values are important and may give us a better fit in our subsequent attempt of reconstructing the action potential from the separated ionic currents [2, 24].

The shape of an action potential evoked by activation of the F Na current was demonstrated after a block of all other currents [40]. Cells of F current have an action potential of a low threshold, rapid rate of rise, and short duration. Their kinetics of inactivation prevent neurons with this current from spontaneously firing repetitively. However, neurons with F current follow high frequency stimulation. Such neurons, with an appropriate high sensitivity to TTX, are abundant among the DRG cells, and are denoted F neurons by some investigators [39, 67], and low threshold by others [16, 39, 40].

The action potentials of cells with S currents have higher threshold, slower rate of rise, and longer duration than F neurons. Due to their slow kinetics of inactivation and their depolarized Vh_{50}, cells of these currents fire repetitively, but have limited ability to follow high frequency stimulation. Such cells, with low sensitivity to TTX, are also identified among the DRG population [10].

The shape of the action potential of cells with intermediate (I) currents is between the fast and slow ones [40]. The presence of neurons with F, S and I currents enlarges the spectrum of firing patterns among the DRG neurons, compared to the "basic firing pattern" expected in a population of DRG neurons with only the I current. Thus, NGF was found to have the important role of accelerating the development of a diverse firing spectrum among maturing DRG neurons, compared to the stereotypic forming of a "basic neuron" [10] in DRG cells grown in NGF-free conditions.

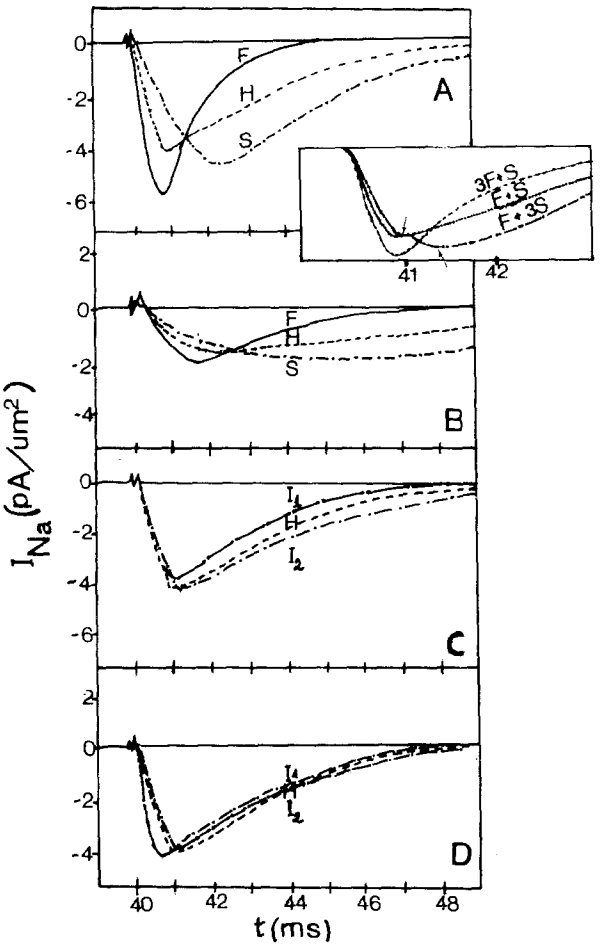

Fig. 7. "Hybridization" of a fast and slow currents. (*A*) and (*B*) Traces of a fast (*F*)-cell (smooth line, cell G225R) and a slow (*S*)-cell (dashed-dotted line, cell G230V) were depicted from two cells depolarized to −10 mV (*A*) or −25 mV (*B*). The traces were mixed at 1 : 1 ratio to yield the hybrid (*H*) (dotted line) which resembles trace of an intermediate cell. (*C*) The hybrid line of *A* and *B* above (*H*) is depicted along with current traces of two intermediate cells (G186J (I_1)- dashed-dotted line, and G509C (I_2)- dashed-dotted line) of the −NGF groups depolarized to −10 mV. The hybrid line was scaled to fit current amplitude of the measured currents. (*D*) As in *C*, but current traces were obtained from two cells cultured with NGF (G334L (I_1)- dashed-dotted line, G371V (I_2)- dashed line). Again, the hybrid trace (*H*) was scaled to fit peak currents of the measured traces. Inset: hybridization of the *F* and *S* currents of *A* at various ratios: $F:S = 3:1$, dashed line; $F:S = 1:1$, dotted line; and $F:S = 1:3$, dashed-dotted line. Note the differences in time to peak, kinetics of inactivation, and the implied presence of two current peaks (arrows) in the $F:S = 1:3$ curve. All cells were cultured for 6–9 hr

Current Diversity and Channel Diversity

F and *S* currents differ significantly from each other in their voltage dependency of activation, inactivation and kinetics. They also have different TTX sensitivities. *I* current appears to be a simple combination of the two. However, single-channel recording is required to verify whether *I* is not generated by a third channel type [21]. It is interesting that the properties of each current were not altered over time in culture. The developmental process seems to progress in the direction of creating different combinations from the two available current types, rather then forming multiple types of currents. NGF was important in accelerating the development of such current diversity.

F and *S* sodium currents are predicted to be carried by different molecular complexes of the Na channel. They may have different primary sequences [29, 44, 45, 65], various levels of subunit oligomerization [32, 43], or arise as a result of post-translational changes [4]. The differing TTX sensitivities of the three currents are noteworthy in this context. Although most Na channels are TTX sensitive, the presence of TTX-insensitive channels was previously described for denervated and developing skeletal and heart muscles [66], molluscan neurons, sympathetic neurons [27], and the TTX-producing fish [21]. TTX insensitivity is always associated with slow kinetics [27, 61, 66]. Trypsin treatment was also found capable of artificially generating a TTX-resistant slow current [34]. However, our results show that *S* and *I* currents are present in cells cultured without exposure to trypsin, suggesting that these are native currents.

To identify the TTX-insensitive channel as a sodium channel, the $[Ca]_{out}$ test was employed. This test was developed [1, 8, 17] to reveal the presence of calcium binding sites within the calcium channels, and to elucidate their role in regulating calcium channel permeability, selectivity, and gating [1, 8, 17, 30, 37]. In our study it was used as a screening assay to differentiate between sodium and calcium channels, and found effective in distinguishing between the two channels.

The effect of $[Ca]_{out}$ on the *S* current in our study is consistent with its previously reported effects on *S* sodium currents described for other cells of neural crest origin [27]. We went one step further and characterized the effect of $[Ca]_{out}$ on TTX affinity to *S* and *F* channels. In the classical channels, TTX and calcium compete for a binding site at the selectivity filter of the TTX-sensitive Na channel [18, 22]. We confirmed these observations for the *F*, TTX-sensitive site. However, the opposite was discovered for the *S*, TTX-insensitive Na current in which Ca was found to increase the affinity to TTX. A more detailed examination of this assay on a larger spectrum of TTX-insensitive neurons may reveal how general this finding is, and whether it can

be used to elucidate the structure of the TTX-insensitive Na channel.

The Effect of NGF on Na Current

Adding NGF to defined culture medium in our study resulted in: (*i*) earlier presence of Na currents, (*ii*) earlier appearance of *S* and *F* cells leading to an increase in the diversity of sodium currents, and (*iii*) an increase in the density of the Na current due to earlier appearance of neurons with larger Na current density (the *F* and *S* types). Thus, the main effect of NGF is to accelerate the acquisition of the various Na currents. It appears that in the absence of NGF, cells are not yet committed and develop both *S* and *F* currents mixed together at low density within a single cell. Then, as a function of time, and more rapidly with NGF, one current proliferates and dictates the nature of the cell. Whether this reflects an increase in single-channel current, or an increase in channel number, remains to be determined by single-channel recording. The results of this study are insufficient to tell whether turning of *I* into either *F* or *S* cell is a function of a genetic preprogram, a possible difference in the cascade of responses to NGF, or the consequence of the involvement of another environmental factor(s).

The action of NGF in increasing the diversity of Na currents among the DRG cells can produce a diversity of excitability and firing patterns suitable to the large spectrum of sensory information which the peripheral neurons are required to handle [12, 15, 16, 40, 59]. However, NGF acts only on the rate at which such diversity is developed. When neurons are cultured without NGF, Na current diversity is still developed, but over a longer period of time, suggesting that the diversity is an inherent feature of the sodium current in the DRG cells, and NGF sets the clock.

The finding that NGF affects the time onset of the currents and their diversity, and does not modify the current properties once established, coincides with what is known today about the in vivo development of Na currents and Na-dependent action potentials among mammalian DRG cells. Studies performed *in situ* [15, 16] and on neurons obtained fresh from the animal demonstrated that it is the proportion of neurons with each type of action potential that is changing during development [39, 59, 67]. The DRG's of frogs and chicks exhibit only one current type throughout development [10, 45]. The presence of two types of Na currents in the mammalian sensory neurons, and their diversified distribution, may have importance in the generation of a larger spectrum of firing in response to various types of stimulation. Also, the distribution of *F* and *S* channels in a neuron can be nonhomogeneous [4], providing another level of specialization [4].

The lumbar and sacral neurons of the DRG (and also within each ganglion) are generated over a period of several days [35, 53], and the ganglia of newborns contain a mixture of mature and immature cells [53]. It is possible that whether a neuron becomes *F* or *S* is related to its age. Indeed, DRG neurons obtained from 16-day-old embryos have no pure *S* neurons [68; I. Zeitoun, *personal communication*]. However, we cannot rule out the possibility that there are different neuronal precursors for *F* and *S* cells [7, 10]. The *F* or *S* nature of the neuron may also be dictated by the target the neuron was connected to in the animal, before being isolated into culture [53, 58, 59].

The response of DRG sodium currents to NGF can be compared to the response of the pheochromocytoma PC_{12} cells. The addition of NGF to PC_{12} cells was followed by increased electrical excitability [6] due to elevated number and density of TTX-sensitive sodium channels, and the appearance of a few neurons with TTX-insensitive "Na-spikes" [6, 38, 48, 56]. Considering the common embryonic origin, it is reasonable to generalize that channel diversity is under NGF regulation in mammalian neural crest-derived cells. There are differences, however, between DRG and PC_{12}: the effect in DRG takes a few hours compared to several days in PC_{12} [38]; the DRG cells exhibit a larger proportion of neurons with *S*, TTX-insensitive Na current [56]; and NGF works in DRG cells mainly on the rate of the processes, while it works in PC_{12} cells on the final current density [38]. Since PC_{12} are transformed cells, these differences can be attributed to the transformation process.

How does the effect of NGF develop? Four different mechanisms are postulated: (*i*) selective survival of neurons, (*ii*) enhanced synthesis of *S* and *F* channels, (*iii*) DNA activation via promoters and enhancers, and (*iv*) active post-translational modification of channels.

Selective Survival

This model suggests a linkage between the effect of NGF on selective survival of subgroups of neurons [7, 53] and the development of a particular type of Na current in their membrane. Our results do not support this model, since there were no significant differences in the survival of neurons with and without NGF (Table 2). The measurements of survival were taken 1 hr after disaggregating the neurons to

single cells, with and without NGF. If NGF worked via selective survival, the entire process would have to be completed within 1 hr—an unusually short time for differentiation processes regulated by NGF [60].

Enhanced Synthesis of F and S Channels

NGF may work at the mRNA level to enhance the synthesis of Na channels [38]. If so, according to our study, NGF would have to enhance the synthesis of *F* or *S* channels in 2–6 hr. Indeed, it was found that mammalian neurons cultured at 37°C require only 2–6 hr to take up labeled amino acids, synthesize channels, and complete the incorporation of TTX-sensitive sodium channels to the plasma membrane [57]. Thus, it is possible that if NGF enhances the synthesis of Na channels, these channels can be detected within several hours of growth with NGF.

DNA Level

It was found that NGF in PC_{12} cells stimulates the transcription of c-fos oncogenes associated with NGF ability to induce outgrowth and increase Na channel density [33]. Thus, it is possible that the effect of NGF on Na currents is mediated at the DNA level.

Post-Translational Modulation

It is well known that chemical modifications can change TTX sensitivity, and that these modifications are often associated with slowing current kinetics [54, 61]. NGF cannot be included among these factors, since it does not change the characteristics of the currents, and has no acute effect on current properties. The binding of NGF to its receptor may, however, activate second messenger systems, thereby changing protein phosphorylation and methylation [13, 52]. NGF is capable of activating Ca channels [64] and changing the level of intracellular calcium [11, 58]. Second messengers and intracellular calcium were found to change Na current density and, to a lesser extent, to modify their voltage dependency or TTX sensitivity [4]. Thus, they may affect the differentiation towards either *S* or *F* current (depending on the cellular cascade which is activated in a cell). Rang and Ritchie [55] found a TTX-resistant, slow Na channel in rat sensory nerves, which is recruited following permanent activation of protein kinase C by second messengers. At the same time, the TTX-sensitive channels were suppressed. (Interestingly, the TTX-insensitive Na channel they found is also depressed by millimoles of external calcium like our *S* current.) NGF receptors may serve as the potential surface molecules linking second messengers to processes regulating the acquisition of Na currents [11, 19, 33].

The relatively simple approach of short-duration culturing in serum-free defined medium, and patch clamping, enabled us to start eliminating some of the possibilities listed above. Further studies employing inhibitors of protein synthesis, RNA translation or DNA transcription, as well as the use of activators of second messengers [4, 33, 38, 52, 55] may illuminate the level(s) at which NGF is working.

We are grateful to Professor Y. Palti for his help in the design and analysis of these experiments and his comments on the manuscript. We thank A. Schwartz and O. Adler for their contribution to the TTX and Ca experiments; Dr. D. O'Dowd for her part in establishing the experiments on the DRG system; S. Magar for adapting the analysis programs to the MV-2000 computer; N. Topolev for her enormous help in computer analysis; Y. Rosenthal and R. Shatzberger for many useful discussions; and I. Zeitoun for providing unpublished data on the development of Na current in vivo in serum-containing medium. This research was supported by the US-Israel Bi-National Science Foundation (No. 84-00367) and a basic research grant from the Israel Academy of Sciences (No. 480.87).

References

1. Almers, W., McCleskey, E.W. 1984. Non-selective conductance in calcium channels of frog muscle: Calcium selectivity in a single-file pore. *J. Physiol. (London)* **353:**585–608
2. Armstrong, C. 1981. Sodium currents and gating currents. *Physiol. Rev.* **61:**644–683
3. Bossu, J.L., Feltz, A. 1984. Patch-clamp study of the tetrodotoxin-resistant sodium current in group C sensory neurons. *Neurosci. Lett.* **51:**241–246
4. Catterall, W.A. 1988. Structure and function of voltage sensitive ion channels. *Science* **242:**50–61
5. Cohen, S., Levi-Montalcini, R. 1956. A nerve growth stimulating factor isolated from snake venom. *Proc. Natl. Acad. Sci. USA* **42:**571–574
6. Dichter, M.A., Tischler, A.S., Green, L.A. 1977. Nerve growth factor induced increase in electrical excitability and acetylcholine sensitivity of a rat pheochromocytoma cell line. *Nature (London)* **268:**561–564
7. Edgar, D., Barde, Y.A., Thoenen, H. 1981. Subpopulations of cultured sympathetic neurons differ in their requirements for survival factors. *Nature (London)* **289:**294–295
8. Fedlova, S.A., Kostyuk, P.G., Vaselovsky, N.S. 1985. Two types of calcium currents in the somatic membrane of newborn rat dorsal root ganglion neurons. *J. Physiol. (London)* **359:**431–446
9. Fenton, E.L. 1970. Tissue culture assay of nerve growth factor and of the specific antiserum. *Exp. Cell Res.* **59:**383–392

10. Gottman, K., Dietzel, I.D., Lux, H.D., Huck, S., Rohrer, H. 1988. Development of inward currents in chick sensory and autonomic neuronal precursor cells in culture. *J. Neurosci.* **8**:3722–3733
11. Gundersen, R.W., Barrett, J.N. 1980. Characterization of the turning response of dorsal root neurites towards nerve growth factor. *J. Cell. Biol.* **87**:546–554
12. Guyton, A.C. 1981. Medical Physiology. Chap. 48, p. 595. Sounders, Philadelphia
13. Halegoua, S., Patrick, J. 1980. Nerve growth factor mediates phosphorylation of specific proteins. *Cell* **22**:571–581
14. Hamill, O.P., Marty, A., Neher, E., Sakman, B., Sigworth, F.J. 1981. Improved patch clamp techniques for high-resolution current recording from cells and cell free membrane patches. *Pfluegers Arch.* **391**:85–100
15. Harper, A.A., Lawson, J.N. 1985. Conduction velocities related to morphological cell type in rat dorsal root ganglia. *J. Physiol. (London)* **359**:31–46
16. Harper, A.A., Lawson, J.N. 1985. Electrical properties of dorsal root ganglion neurons with different peripheral nerve conduction velocities. *J. Physiol. (London)* **359**:47–63
17. Hess, P., Lansman, J.B., Tsien, R.W. 1986. Calcium channel selectivity for divalent and monovalent cations. *J. Gen. Physiol.* **88**:293–319
18. Henderson, R., Ritchie, J.M., Strichartz, G.R. 1984. Evidence that tetrodotoxin and saxitoxin act at a metal cation binding site in the sodium channel of nerve membrane. *Proc. Natl. Acad. Sci. USA* **71**:3936–3940
19. Heumann, R., Lindholm, D., Bandtlow, C., Meyer, M., Radeke, M., Misko, T.P., Shooter, E., Thoenen, H. 1987. Differential regulation of mRNA encoding nerve growth factor and its receptor in rat sciatic nerve during development, degeneration and regeneration: Role of macrophages. *Proc. Natl. Acad. Sci. USA* **84**:8735–8739
20. Heyer, E.J., McDonald, R.L. 1982. Calcium and sodium dependent action potentials of mouse spinal cord and dorsal root ganglion neurons in cell culture. *J. Neurophysiol.* **47**:641–655
21. Hille, B. 1984. Ionic Currents of Excitable Membrane. Sinauer, Sunderland (MA)
22. Hille, B., Ritchie, J.M., Strichartz, G.R. 1975. The effect of surface charge on the nerve membrane and on the action of tetrodotoxin and saxitoxin in frog myelinated nerve. *J. Physiol. (London)* **250**:34p–35p
23. Hille, B., Woodhull, A.M., Shapiro, B.I. 1975. Negative surface charge near sodium currents of nerve: Divalent ions, monovalent ions and pH. *Philos. Trans. R. Soc. London B* **270**:301–318
24. Hodgkin, A.L., Huxley, A.F. 1952. A quantitative description of membrane currents and its application to conduction and excitation in nerve. *J. Physiol. (London)* **117**:500–544
25. Honegger, P., Lenoir, D. 1982. Nerve growth factor (NGF) stimulation of aggregating cell cultures. *Dev. Brain Res.* **3**:229–238
26. Honegger, P., Lenoir, D., Faurod, P. 1979. Growth and differentiation of aggregating fetal brain cells in serum-free defined medium. *Nature (London)* **282**:305–307
27. Ikeda, S.R., Schofield, G.G. 1987. Tetrodotoxin resistant sodium current at nodose neurons; monovalent cation selectivity and divalent cation block. *J. Physiol. (London)* **389**:255–270
28. Johnson, E.M., Rich, K.M., Yip, H.K. 1986. The role of NGF in sensory neurons in-vivo. *Trends Neurosci.* **9**:33–37
29. Kayano, T., Noda, M., Flockerzi, V., Takahashi, H., Numa, S. 1988. Primary structure of rat brain sodium channel III deduced from the cDNA sequence. *FEBS. Lett.* **228**:187–194
30. Kostyuk, P.G., Shuba, Ya.M., Savahenko, A.N. 1988. Three types of calcium currents in the membrane of mouse sensory neurons. *Pfluegers Arch.* **411**:661–669
31. Kostyuk, P.G., Vaselovsky, N.S., Tsynderenko, A.Y. 1981. Ionic currents in the somatic membrane of the rat dorsal root ganglion neurons. I. Sodium currents. II. Calcium currents. *Neuroscience* **6**:2423–2438
32. Krafte, D.S., Snutch, T.P., Leonard, J.P., Davidson, N., Lester, H.A. 1988. Evidence for the involvement of more than one mRNA species in controlling the inactivation process of rat and rabbit brain Na channels expressed in *Xenopus* oocytes. *J. Neurosci.* **8**:2859–2868
33. Kremer, N.E., Brugge, J.S., Halegoua, S. 1989. Inhibition by anti-SRC and anti-RAS antibodies of PC_{12} differentiation by nerve growth factor and basic fibroblast growth factor. Proceedings of the 8th Annual Stony Brook Symposium on Recent Advances in Molecular Neurobiology. p. 12
34. Lee, K.S., Akaike, N., Brown, A.M. 1977. Trypsin inhibits the action of tetrodotoxin on neurones. *Nature (London)* **265**:751–753
35. Levi-Montalcini, R., Angeletti, P.U. 1963. Essential role of the nerve growth factor in the survival and maintenance of dissociated sensory and sympathetic embryonic cells in vitro. *Dev. Biol.* **7**:653–659
36. Levi-Montalcini, R., Mugnaini, A.E., Oesch, F., Thoenen, H. 1975. Nerve growth factor induces volume increase and enhances tyrosine hydroxylase synthesis in chemically axotomized sympathetic ganglia of newborn rats. *Proc. Natl. Acad. Sci. USA* **72**:595–599
37. Lux, M.D., Carbone, E., Zucker, H. 1989. Block of Na ion permeation and selectivity of calcium channels. *Ann. N.Y. Acad. Sci.* **560**:94–102
38. Mandel, G., Cooperman, S.S., Maue, R.A., Goodman, R.H., Brehm, P. 1988. Selective induction of brain type II Na channels by nerve growth factor. *Proc. Natl. Acad. Sci. USA* **85**:924–928
39. Matsuda, Y., Yoshida, S., Yonezawa, T. 1978. Tetrodotoxin sensitivity and calcium component of action potentials of mouse dorsal root ganglion cell cultured in-vitro. *Brain Res.* **154**:69–82
40. McLean, M.J., Bennet, P.B., Thomas, R.M. 1988. Subtypes of dorsal root ganglion neurons based on different inward currents as measured by whole cell voltage clamp. *Mol. Cell. Biochem.* **80**:95–107
41. Meiri, H., Omri, G., Zeitoun, I., Savion, N. 1986. Environmental factors that influence the differentiation, and the development of voltage dependent sodium channels in cultured dorsal root ganglion cells of newborn rats. *Exp. Brain Res. Suppl.* **13**:231–245
42. Meiri, H., Spira, G., Sammar, M., Namir, M., Schwartz, A., Komoriya, A., Kosower, E.M., Palti, Y. 1987. Mapping a region associated with Na channel inactivation using antibodies to synthetic peptide corresponding to a part of the channel. *Proc. Natl. Acad. Sci. USA* **84**:5058–5062
43. Messner, D.J., Feller, D.J., Scheuer, T., Catterall, W.A. 1986. Functional properties of rat brain sodium channel lacking the $betha_1$ or $betha_2$ subunits. *J. Biol. Chem.* **26**:14882–14890
44. Noda, M., Ikeda, T., Kayano, T., Suzuki, H., Takeshima, H., Kurasaki, M., Takahashi, H., Numa, S. 1985. Existence of distinct sodium channel messengers RNA in rat brain. *Nature (London)* **320**:188–192

45. O'Dowd, D.K., Aldrich, R.W. 1988. Voltage clamp analysis of sodium channels in wild type, and mutant *Drosophila* neurons. *J. Neurosci.* **8**:3633–3643
46. O'Dowd, D.K., Ribera, A.B., Spitzer, N.C. 1987. Development of voltage-dependent calcium, sodium, and potassium currents in *Xenopus* spinal neurons. *J. Neurosci.* **8**:792–805
47. Okun, L.M. 1972. Isolated dorsal root ganglion neurons in culture: Cytological maturation and extension of electrically active processes. *J. Neurobiol.* **3**:111–151
48. O'lague, P.H., Huttner, S.L., Vandenberg, C.A., Morrison-Graham, K., Horn, R. 1985. Morphological properties, and membrane channel of the growth cones induced in PC_{12} cells by nerve growth factor. *J. Neurosci. Res.* **13**:301–321
49. Orozco, C.B., Epstein, C.J., Rapoport, S.I. 1988. Voltage activated sodium conductance in cultured normal, and trisomy 16 dorsal root ganglion neurons from fetal mouse. *Dev. Brain Res.* **3**:265–274
50. Palti, Y., Adelman, W.J. 1969. Measurements of axonal membrane conductances, and capacity by means of varying potential control voltage clamp. *J. Membrane Biol.* **1**:431–458
51. Palti, Y., Cohen-Armon, M. 1982. Numerical method for correcting the series resistance error in voltage clamp experiments. *Isr. J. Med. Sci.* **18**:19–24
52. Pfenninger, K.H., Johnson, M.P. 1981. Nerve growth factor stimulates phospholipid methylation in growing neurites. *Proc. Natl. Acad. Sci. USA* **78**:7797–7800
53. Purves, D., Lichtman, J.W. 1985. Principles of Neuronal Development. Chap. 7. Trophic effects of targets on neurons. pp. 155–178. Sinauer, Sunderland (MA)
54. Rack, M., Rubly, N., Waschow, C. 1986. Effects of some chemical regents on sodium current in myelinated nerve fibers of the frog. *Biophys. J.* **50**:557–564
55. Rang, H.P., Ritchie, J.M. 1988. Depolarization of non-myelinated fibers of the rat vagus nerve produced by activation of protein kinase C. *J. Neurosci.* **8**:2606–2617
56. Rudy, B., Kirschenbaum, B., Green, L.A. 1987. Nerve growth factor increase the number of functional Na channels, and induces TTX resistant Na channels in PC_{12} pheochromocytoma cells. *J. Neurosci.* **7**:1613–1625
57. Schmidt, J., Rossie, S., Catterall, W.A. 1985. A large intracellular pool of inactive Na channel alpha subunits in developing rat brain. *Proc. Natl. Acad. Sci. USA* **82**:4847–4851
58. Schwab, M.E., Heumann, R., Thoenen, H. 1982. Communication between target organs, and nerve cells: Retrograde axonal transport, and site of action of nerve growth factor. *Cold Spring Harbor Symp. Quant. Biol.* **46**:125–134
59. Scott, B.S., Edwards, B.A.V. 1980. Electric membrane properties of adult mouse DRG neurons, and the effect of culturing duration. *J. Neurobiol.* **11**:291–301
60. Server, A.C., Shooter, E.M. 1977. Nerve growth factor. *Adv. Protein Chem.* **31**:339–409
61. Spalding, B.C. 1980. Properties of toxin resistant sodium channels produced by chemical modification in frog skeletal muscles. *J. Physiol. (London)* **305**:485–500
62. Spitzer, N.C. 1979. Ion channels in development. *Annu. Rev. Neurosci.* **2**:363–397
63. Stolc, S., Nemcek, V., Boska, D. 1988. Potential clamp of isolated dialyzed neuron: Minimalization of the effect of series resistance. *Gen. Physiol. Biophys.* **7**:303–312
64. Streit, J., Lux, H.D. 1988. Calcium current distribution in PC_{12} cells during NGF-induced differentiation. *Pfluegers Arch.* **411 (Suppl. R)**:143
65. Stuhmer, W.C., Methfessel, C., Sakmann, B., Noda, M., Numa, S. 1987. Patch clamp characterization of sodium channels expressed from rat brain cDNA. *Eur. Biophys.* **14**:131–138
66. Weiss, R.E., Horn, R. 1986. Functional differences between two classes of sodium currents in developing rat skeletal muscle. *Science* **233**:361–364
67. Yoshida, S., Matsuda, Y., Samejima, A. 1978. Tetrodotoxin-resitant sodium, and calcium component of action potentials in DRG cells of the adult mouse. *J. Neurophysiol.* **41**:1096–1106
68. Zeitoun, I., Meiri, H., Omri, G., Palti, Y. 1987. The development of different types of sodium channels in rat DRG cells. *Proc. Int. Biophys. Congr.* **9**:143

Received 27 March 1989; revised 19 October 1989